

# Influence of uniaxial stress on the lamellar spacing of eutectics

Jens Kappey\*, Klaus Kassner\* and Chaouqi Misbah\*\*

\* *Institut für Theoretische Physik, Otto-von-Guericke-Universität  
Magdeburg, Postfach 4120, D-39016 Magdeburg, Germany*

\*\* *Laboratoire de Spectrométrie Physique, Université Joseph Fourier (CNRS),  
Grenoble I - B.P. 87, 38402 Saint-Martin d' Hères Cedex, France*

Directional solidification of lamellar eutectic structures submitted to uniaxial stress is investigated. In the spirit of an approximation first used by Jackson and Hunt, we calculate the stress tensor for a two-dimensional crystal with triangular surface, using a Fourier expansion of the Airy function. The effect of the resulting change in chemical potential is introduced into the standard model for directional solidification. This calculation is motivated by an observation, made recently [I. Cantat, K. Kassner, C. Misbah, and H. Müller-Krumbhaar, Phys. Rev. E, in press], that the thermal gradient produces similar effects as a strong gravitational field in the case of dilute-alloy solidification. Therefore, the coupling between the Grinfeld and the Mullins-Sekerka instabilities becomes strong, as the critical wavelength of the former instability gets reduced to a value close to that of the latter. Analogously, in the case of eutectics, the characteristic length scale of the Grinfeld instability should be reduced to a size not extremely far from typical lamellar spacings. Following Jackson and Hunt, we assume the selected wavelength to be determined by the minimum undercooling criterion and compute its shift due to the external stress. In addition, we find that in general the volume fraction of the two solid phases is changed by uniaxial stress. Implications for experiments on eutectics are discussed.

81.10.Aj,05.70.Ln,81.40.Jj,81.30.Fb

## I. INTRODUCTION

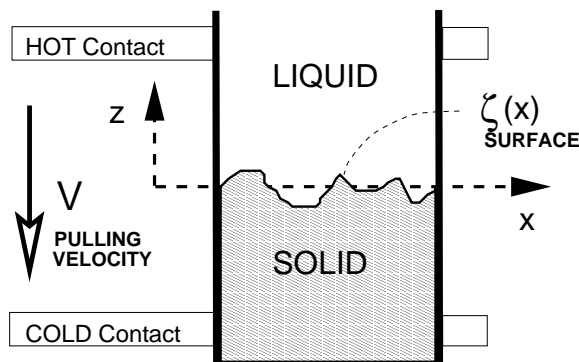


FIG. 1. Schematic setup of a directional solidification experiment. A container with the melt in it is pushed through a thermal gradient  $G$  with a velocity  $V$ .

A non-hydrostatically strained solid in contact with its melt or vapor can partially relieve its elastic energy by producing an undulated interface. This is the cause of a morphological instability giving rise to the evolution of grooves with a definite spacing under uniaxial stress and, possibly, island formation, if the stress is biaxial. The instability was first predicted by Asaro and Tiller [1]. Experimentally, it has been observed and studied by Torii and Balibar [2]. Since the independent rediscovery of the instability by Grinfeld [3], it has often been referred to as the Grinfeld or Asaro-Tiller-Grinfeld instability (ATG). Important contributions leading to a broad interest in the instability are due to Nozières [4,5].

In directional solidification (Fig.1), it is known that the moving front undergoes, depending on the growth velocity, another morphological instability, named after Mullins and Sekerka [6] (MS), where the interface develops a cellular structure. Cantat *et al.* [7,8] investigated the coupling between these two instabilities for dilute alloys.

They discovered that under favourable circumstances a weak uniaxial stress of the order of 1 bar leads to a dramatic change in the stability range of the Mullins-Sekerka instability. A schematic representation of one of the most common liquid-solid equilibrium phase diagrams is displayed in Fig 2. Dilute alloy means that the concentration of the minor phase is very small. The other situation, in which we are interested here, corresponds to a composition close to the eutectic one. The growing solid then often forms a parallel array of the two coexisting phases  $\alpha$  and  $\beta$  that grow side by side. This growth mode is called lamellar eutectic growth.

A seminal theoretical description of lamellar eutectics has been given by Jackson and Hunt (JH) [9]. Their basic idea is the replacement of the diffusion field in the liquid phase with that of a planar front. Assuming that the  $\alpha$  and  $\beta$  lamellas have equal average undercoolings they were able to obtain an analytic approximation for the average undercooling of the interface. They then invoked the hypothesis, which has since become known as *minimum undercooling assumption*, that the *selected* wavelength of the pattern leads to the minimum possible value of the undercooling (which means that for *given* undercooling the *fastest-growing* structure is selected).

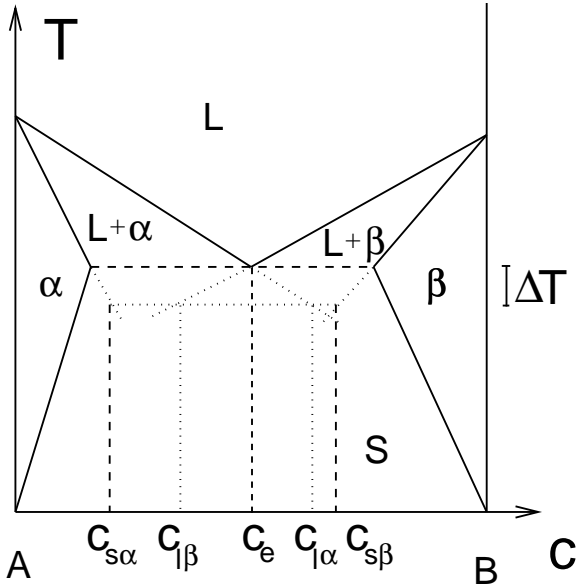


FIG. 2. Generic phase diagram of a binary eutectic.  $T$  is the temperature,  $c$  the concentration of one component. The regions  $L$ ,  $\alpha$ , and  $\beta$  correspond to one-phase equilibrium states of the liquid, the solid  $\alpha$ , and the solid  $\beta$  phases, respectively.  $L+\alpha$  and  $L+\beta$  are regions of two-phase equilibrium between the liquid and the solid phases; the actual concentrations of the two phases are given by the liquidus and solidus lines (full lines) delimiting these regions.  $c_e$ ,  $c_\alpha$ , and  $c_\beta$  denote the equilibrium concentrations of the liquid and the two solid phases at the triple or eutectic point. The concentrations for the undercooled case are also displayed.

## II. MODEL EQUATIONS

In describing the problem by a macroscopic continuum model we must introduce fields. These are the temperature, the concentrations and the stress fields. We make some standard simplifying assumptions about the properties of the system, believed not to affect its essential physical features. These simplifications were justified elsewhere [10]. For the sake of completeness, we recapitulate them briefly. The thermal gradient  $G$  is assumed constant in the frame of reference moving along with the growing interface. This means that thermal diffusion is much faster than chemical diffusion, that thermal conductivities of all phases are equal, and that latent heat production can be neglected. Thanks to this approximation, the motion of the temperature field is completely decoupled from that of the concentration field. Temperature is given by position, which effectively reduces the number of fields to be considered by one. We further suppose the attachment kinetics at the solid-liquid interface to be fast on the time scales of all other transport processes. This assumption is legitimate for microscopically rough interfaces. We take surface tension to be isotropic. In the vicinity of the operating point in the phase diagram, the slopes of the liquidus and the solidus line are

assumed constant. This leads to temperature independent partition coefficients for both phases  $\alpha$  and  $\beta$ . The partition coefficients  $k_{\alpha/\beta}$  are the ratios of the slopes of the liquidus and solidus lines, respectively. In addition, we restrict ourselves to the so called one-sided model, i.e., we have no diffusion in the solid phases.

Introducing a dimensionless concentration field  $c = (\tilde{c} - \tilde{c}_e)/\Delta\tilde{c}$ , where  $\tilde{c}$  stands for the physical concentration and  $\Delta\tilde{c} = \tilde{c}_\beta - \tilde{c}_\alpha$  is the miscibility gap, we can write the equation of motion in the laboratory frame (where the sample is pushed at constant velocity  $V$  along the  $-z$  direction)

$$\nabla^2 c + \frac{2}{l} \frac{\partial c}{\partial z} = 0. \quad (1)$$

In this equation,  $l = 2D/V$  is the diffusion length, where  $D$  is the diffusion constant. One boundary condition for the diffusion equation takes into account that the concentration far away from the surface has a constant value  $c_\infty = (\tilde{c}_\infty - \tilde{c}_e)/\Delta\tilde{c}$ . In the lateral direction, we assume periodic boundary conditions:  $c(x, z) = c(x + \lambda, z)$ . Mass conservation requires boundary conditions for the normal derivatives of the concentration fields at the liquid-solid interface. This continuity equation reads

$$-D \frac{\partial c}{\partial n} \Big|_{\text{Interface}} = \begin{cases} ((1 - k_\alpha)c + \delta)v_n \\ ((1 - k_\beta)c + \delta - 1)v_n \end{cases} \quad (2)$$

where  $\delta = (\tilde{c}_e - \tilde{c}_\alpha)/\Delta\tilde{c}$  is the reduced miscibility gap of the  $\alpha$  phase and  $1 - \delta$  that of the  $\beta$  phase.  $v_n = (2D/l + \zeta(x))n_z$  is the normal velocity of the interface where the normal points from the solid into the liquid.

For the stress field we impose mechanical equilibrium,  $\sum_j \partial \sigma_{ij} / \partial x_j = 0$ , which means that on the time scale of the concentration field, the stress is always relaxed. We assume linear elasticity and an isotropic solid, so that Hooke's law reads:

$$\sigma_{ij} = \frac{E_{\alpha/\beta}}{1 + \nu_{\alpha/\beta}} (u_{ij} + \frac{\nu_{\alpha/\beta}}{1 - 2\nu_{\alpha/\beta}} u_{kk} \delta_{ij}), \quad (3)$$

where  $\sigma_{ij}$  are the components of the stress tensor and  $u_{ij} = \frac{1}{2}(\partial u_i / \partial x_j + \partial u_j / \partial x_i)$  those of the strain tensor ( $u_i$  is the displacement vector).  $E_\alpha$  ( $E_\beta$ ) is Young's modulus for the  $\alpha$  ( $\beta$ ) phase,  $\nu_\alpha$  ( $\nu_\beta$ ) the Poisson number.

The boundary conditions at the solid-liquid interface are

$$\begin{aligned} \sigma_{nn} &= \mathbf{n} \sigma \mathbf{n} = -p_l, \\ \sigma_{nt} &= \mathbf{n} \sigma \mathbf{t} = 0, \end{aligned} \quad (4)$$

where  $\mathbf{n}$  ( $\mathbf{t}$ ) is the normal (tangential) vector at the interface, and  $p_l$  is the pressure in the liquid. These conditions state that we have no shear at the solid-liquid boundary and that the normal component of the stress tensor is continuous. That is, we neglect the capillary overpressure present when the interface is curved. Usually, this is a good approximation.

There are two further points that have to be taken into account. Both result from the requirement of local thermodynamic equilibrium at the interface, due to fast interface kinetics. The first of these is often referred to as ‘mechanical’ equilibrium condition for the surface tensions of the three interfaces meeting at a triple point (although it is indeed a condition of thermodynamic equilibrium under particle exchange, i.e., one of chemical equilibrium). The contact angles  $\vartheta_{\alpha/\beta}$  (see Fig.3) should obey

$$\begin{aligned} \gamma_{\alpha l} \sin \vartheta_{\alpha} + \gamma_{\beta l} \sin \vartheta_{\beta} &= \gamma_{\alpha\beta}, \\ \gamma_{\alpha l} \cos \vartheta_{\alpha} - \gamma_{\beta l} \cos \vartheta_{\beta} &= 0, \end{aligned} \quad (5)$$

where  $\gamma_{ij}$  is the surface tension between the phases  $i$  and  $j$  (and  $l$  designates the liquid phase).

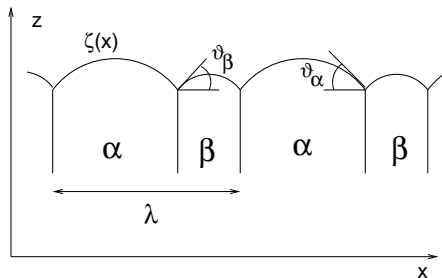


FIG. 3. Illustration of a lamellar eutectic. The interface position is  $z = \zeta(x)$ . The pinning angles  $\vartheta_{\alpha/\beta}$  are also shown.

The second condition couples the stress to the concentration field. It is a modified Gibbs-Thomson equation:

$$\begin{aligned} \epsilon_{\alpha/\beta} c|_{\text{interface}} &= \zeta/l_T^{\alpha/\beta} + d_0^{\alpha/\beta} \kappa \\ &+ H^{\alpha/\beta} \frac{(\sigma_{tt} - \sigma_{nn})^2}{\sigma_0^2}, \\ (\epsilon_{\alpha} &= -1, \quad \epsilon_{\beta} = 1). \end{aligned} \quad (6)$$

In this equation,  $\zeta$  is the  $z$  coordinate of the liquid-solid interface and  $\kappa$  its curvature, taken positive where the solid is convex.  $l_T^{\alpha/\beta}$  are the thermal lengths, given by  $l_T^{\alpha/\beta} = m_{\alpha/\beta} \Delta \tilde{c} / G$ , where  $m_{\alpha}$  ( $m_{\beta}$ ) is the absolute value of the slope of the liquidus line describing coexistence of phase  $\alpha$  ( $\beta$ ) and the liquid.  $d_0^i = \gamma_{il} T_e / L_i m_i \Delta c$  are the capillary lengths ( $i = \alpha, \beta$ ), where  $L_i$  is the latent heat per unit volume and  $T_e$  the eutectic temperature. The modification is the inclusion of the stress term with

$$H^i = \frac{T_e (1 - \nu_i^2) \sigma_0^2}{2E_i |m_i| \Delta c L_i}; \quad i = \alpha, \beta. \quad (7)$$

Herein,  $\sigma_0$  is the uniaxial prestress that can be controlled in experiments. A detailed derivation of eq. (6) is given in [8].

### III. JACKSON-HUNT THEORY FOR A FLAT INTERFACE

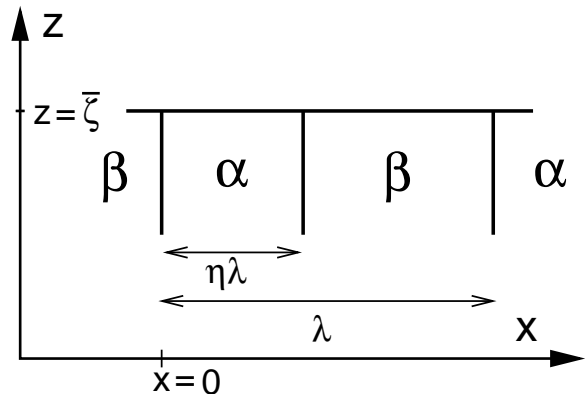


FIG. 4. The flat-interface structure used in the simplest Jackson-Hunt approach.

The first level of approximation in Jackson and Hunt’s approach consisted in replacing the actual diffusion field in (6) with that of a planar lamellar structure sitting at the average position of the solidification front. Without the stress term, (6) would then become a pair of second-order differential equations with boundary conditions following from (5). The solution of these equations with the supplementary condition that the two solutions match at the triple point gives the interface shape and the volume fraction  $\eta$  of the  $\alpha$  phase. Since these equations are nonlinear, they cannot easily be solved analytically. Hence Jackson and Hunt invoked the condition of equal average undercooling of the two solid-liquid interfaces, which fixes the free parameter  $\eta$  and allows to obtain an analytic relation between the average undercooling and the wavelength. The second step – solution for the interface shape – can then be done numerically, if desired.

The main modification in our case is that we have an additional term in (6) involving the stress distribution at the interface. In the spirit of Jackson and Hunt, we compute this expression for a flat interface first. Then the problem becomes very similar to JH’s original approach with the diffusion field replaced by  $c|_i - \epsilon_{\alpha/\beta} H^{\alpha/\beta} (\sigma_{tt} - \sigma_{nn})^2 / \sigma_0^2$ .

Averaging the diffusion field obtained by solving the von-Neumann problem (1), (2) for a flat interface, we have

$$\langle c \rangle_{\alpha} = \frac{1}{k} (c_{\infty} + \delta + \eta - 1) + \frac{2\lambda}{\eta l} P(\eta), \quad (8)$$

$$\langle c \rangle_{\beta} = \frac{1}{k} (c_{\infty} + \delta + \eta - 1) - \frac{2\lambda}{(1-\eta)l} P(\eta), \quad (9)$$

where

$$P(\eta) = \sum_{n=1}^{\infty} \frac{\sin^2(n\pi\eta)}{(n\pi)^3} \quad (10)$$

and the segregation coefficient  $k$  has been taken equal in the two phases. The averages of the curvature of the  $\alpha$  and  $\beta$  lamellas can be obtained without approximation, as they just involve the integration of a derivative,

$$\langle \kappa \rangle_\alpha = \frac{2}{\eta\lambda} \sin \vartheta_\alpha, \quad (11)$$

$$\langle \kappa \rangle_\beta = \frac{2}{(1-\eta)\lambda} \sin \vartheta_\beta. \quad (12)$$

To average the stress terms, we must, in principle, solve the elastic problem for a flat lamellar structure. Innocent as this problem may look, it is not all that trivial. Nevertheless, the final averaging procedure will turn out to be independent of the subtleties that we will now discuss briefly.

At each lamella boundary between the  $\alpha$  and  $\beta$  phases, see Fig. 4, we have, on the one hand, continuity of the normal and shear components of the stress tensor (due to mechanical equilibrium):

$$\begin{aligned} \sigma_{xx}(x=0^-) &= \sigma_{xx}(x=0^+), \\ \sigma_{xz}(x=0^-) &= \sigma_{xz}(x=0^+), \end{aligned} \quad (13)$$

and the same conditions at  $x = \eta\lambda$ . On the other hand, coherence of the interfaces between lamellas imposes additional conditions, viz. continuity of the displacements (up to a constant):

$$\begin{aligned} u_x(x=0^-) &= u_x(x=0^+), \\ u_z(x=0^-) &= u_z(x=0^+), \end{aligned} \quad (14)$$

with again identical conditions at  $x = \eta\lambda$ . Equations (13) and (14) and their counterparts at  $x = \eta\lambda$  constitute two boundary conditions at each vertical boundary for the stress field in the lamella extending between  $x = 0$  and  $x = \eta\lambda$ . (There are four equations but each of them pertains to two lamellas.) The four boundary conditions at the two  $x = \text{const.}$  boundaries of a lamella suffice to solve the elastic problem uniquely. Therefore, there is no room left for more boundary conditions. But in fact, we have, at the boundary towards the liquid

$$\begin{aligned} \sigma_{zz}(z = \bar{\zeta}) &= -p_l, \\ \sigma_{xz}(z = \bar{\zeta}) &= 0, \end{aligned} \quad (15)$$

two additional boundary conditions, rendering the problem overdetermined. Note that this line of reasoning presupposes different elastic constants in the solid phases. If all elastic coefficients are equal, then the validity of (14) implies that of (13) simply by virtue of Hooke's law (assuming, as usual, that continuous physical functions are also continuously differentiable). With different sets of elastic constants in the two phases, we have a situation similar to that in microstructures discussed by Müller [11]. A solution to the elastic problem need not exist. That is, the elastic problem may not have a solution with

the boundaries *fixed* to the chosen positions. However, a solution to the mathematical problem given all the discussed boundary conditions does exist, if we allow the lamella boundaries to adjust their shape, i.e., if we convert the question to a free-boundary problem. The purpose of the following discussion is then only to establish that analytically tractable *homogeneous-stress solutions* exist in *particular* cases.

In fact, we do not need *general* solvability to consider a sensible physical problem. Looking for constant-stress solutions of (14) together with (15) we obtain, setting  $\sigma_{xz}(\bar{\zeta}) = 0$ , the conditions

$$\begin{aligned} -p_l &= \sigma_{zz}^0 = \frac{\nu_\alpha}{1-\nu_\alpha} \sigma_{xx}^0 + \frac{E_\alpha}{1-\nu_\alpha^2} u_{zz}^0, \\ -p_l &= \sigma_{zz}^0 = \frac{\nu_\beta}{1-\nu_\beta} \sigma_{xx}^0 + \frac{E_\beta}{1-\nu_\beta^2} u_{zz}^0, \end{aligned} \quad (16)$$

where the superscript 0 indicates the absence of spatial variation inside the lamellas and the subscripts  $\alpha$  and  $\beta$  distinguish the elastic constants in the two solid phases. There are no such subscripts on the stresses and on  $u_{zz}^0$  which are equal in the two phases (in contrast to  $u_{xx}^0$ , which may differ). It is evident that for different elastic constants in the two materials, (16) has a unique solution for  $\sigma_{xx}^0$  and  $u_{zz}^0$ , providing the coefficient determinant does not vanish. That is, we just have to choose the right value of the prestress  $\sigma_{xx}^0$  to ensure the existence of a homogeneous solution on which we can base our analysis [12]. As long as  $p_l \neq 0$ , we have  $\sigma_{xx}^0 \neq -p_l$ , i.e. the Grinfeld instability is potentially activated. For  $p_l = 0$ , on the other hand, we can even have a continuous set of solutions, if we choose the elastic constants such that the coefficient determinant vanishes (which is possible even for  $E_\alpha \neq E_\beta$ , say).

Given the fact that there is a solution to the elastic problem, the calculation of its influence on the Gibbs-Thomson equation (6) becomes very simple. As  $\sigma_{xx}$  is homogeneous throughout the sample and because of  $\sigma_{tt} = \sigma_{xx}$  for a planar interface, we simply have  $(\sigma_{tt} - \sigma_{nm})^2 / \sigma_0^2 = 1$ . Hence, the averaged stress terms are simply  $H^\alpha$  and  $H^\beta$ , respectively.

Inserting this in the Gibbs-Thomson equation, we get

$$\begin{aligned} \langle \zeta \rangle_\alpha &= \langle \zeta \rangle_\alpha^{JH} + l_T^\alpha H^\alpha, \\ \langle \zeta \rangle_\beta &= \langle \zeta \rangle_\beta^{JH} + l_T^\beta H^\beta, \end{aligned} \quad (17)$$

where  $\langle \rangle^{JH}$  is the average without the stress term. Assuming equal average undercoolings in front of both phases, we set  $\langle \zeta \rangle_\alpha = \langle \zeta \rangle_\beta$ , (because  $\Delta T = -G\zeta$ ). As has been discussed earlier, this assumption is not necessary to obtain closed equations [10], but it simplifies calculations. We can then write an implicit equation for  $\eta$ :

$$\eta = 1 - c_\infty - \delta + k \frac{l_T^\beta H^\beta - l_T^\alpha H^\alpha}{l_T^\alpha + l_T^\beta}$$

$$\begin{aligned}
& + \frac{k}{(l_T^\alpha + l_T^\beta) \eta (1 - \eta)} \left\{ \frac{2\lambda}{l} P(\eta) [\eta l_T^\beta - (1 - \eta) l_T^\alpha] \right. \\
& \left. + \frac{2}{\lambda} [\eta l_T^\beta d_0^\beta \sin \vartheta_\beta - (1 - \eta) l_T^\alpha \sin \vartheta_\alpha] \right\}. \quad (18)
\end{aligned}$$

The last term in this equation is small for small undercooling (implying small Péclet number  $\lambda/l$ ) and small contact angles, so that in this limit an explicit formula for  $\eta$  is available. Using (18) in (17), we obtain for the averaged undercooling:

$$\langle \Delta T(\lambda) \rangle = \langle \Delta T \rangle_{\min} \left( \frac{\lambda}{\lambda_{\min}} + \frac{\lambda_{\min}}{\lambda} \right), \quad (19)$$

where

$$\lambda_{\min} = \lambda_{\min}^{JH}(\eta), \quad (20)$$

$$\langle \Delta T \rangle_{\min} = \langle \Delta T \rangle_{\min}^{JH} + G \frac{l_T^\alpha l_T^\beta}{l_T^\alpha + l_T^\beta} (H^\alpha + H^\beta). \quad (21)$$

Because on setting  $\partial \langle \Delta T \rangle / \partial \lambda = 0$  the elastic terms disappear from the equation for  $\lambda_{\min}$ , there seems at first glance to be no effect of elasticity on the selected wavelength. But that is not true, because  $\eta$  has changed. Expanding  $\lambda_{\min}$  about  $\eta^{JH}$ , setting  $\eta = \eta^{JH} + \Delta\eta$ , we obtain

$$\begin{aligned}
\lambda_{\min} = \lambda_{\min}^{JH}(\eta^{JH}) & \left( 1 + \Delta\eta \left[ -\frac{1}{2} \frac{P'(\eta^{JH})}{P(\eta^{JH})} \right. \right. \\
& \left. \left. + \frac{d_0^\beta \sin \vartheta_\beta - d_0^\alpha \sin \vartheta_\alpha}{\eta^{JH} d_0^\beta \sin \vartheta_\beta + (1 - \eta^{JH}) d_0^\alpha \sin \vartheta_\alpha} \right] \right), \quad (22)
\end{aligned}$$

where  $\Delta\eta \approx k(l_T^\beta H^\beta - l_T^\alpha H^\alpha) / (l_T^\alpha + l_T^\beta)$ .

The first thing to note is that if the elastic constants and the latent heat per volume are equal in the two phases, elastic effects do not influence the wavelength at minimum undercooling, within the flat-interface approximation. This is why we insisted on considering the more general case in spite of the complications concerning the existence of a solution to the elastic problem. The logarithmic derivative  $P'(\eta)/P(\eta)$  of the JH function vanishes for  $\eta = \frac{1}{2}$  and diverges for  $\eta \rightarrow 0$  or  $\eta \rightarrow 1$ , allowing for a potentially large effect. However, it stays smaller than 50 for  $0.04 < \eta < 0.96$ , which means that it does not provide more than an order of magnitude in most situations. The second term in the brackets of (22) usually is on the order of one. The sign of the effect depends on the sign of  $\Delta\eta$ , i.e., the relative magnitude of the elastic constants in the two phases.

If we assume that the difference in Young's moduli in the two phases is on the order of 10% of their average (i.e.,  $(1 - \nu_\beta^2)/2E_\beta - (1 - \nu_\alpha^2)/2E_\alpha \approx 0.05/E_{\text{av}}$ ), we find, for typical values of the material parameters ( $T_e \sim 400\text{K}$ , a freezing range  $m_i \Delta c \sim 10\text{K}$ ,  $L_i \sim 10\text{J/cm}^3$ ,  $k \sim 1$ ,  $E = 10^5 \text{N/cm}^2$ ) and for  $\eta \sim 0.1$  that  $\Delta\eta P'(\eta)/P(\eta) \approx 2 \times 10^{-7} [\text{cm}^4/\text{N}^2] \sigma_0^2$ . This gives a relative wavelength change of  $10^{-5}$  for  $\sigma_0 = 1 \text{bar}$  and one of 10% for  $\sigma_0 = 100$

bar. We therefore conclude that this effect is small in ordinary experiments but might be accessible in high-pressure setups, where pressures of 100 bar or more could be applied.

The next task is then to see what is the order of magnitude of the influence of deviations of the interface shape from planarity.

#### IV. JACKSON-HUNT THEORY FOR A TRIANGULAR INTERFACE

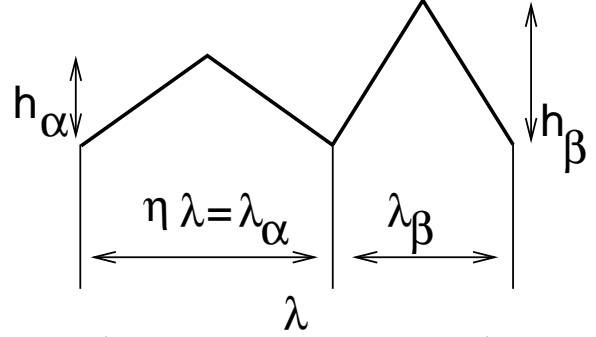


FIG. 5. Simplified surface structure

The simplest non-planar surface structure accessible to an analytic approach is a triangular surface (see Fig 5). To proceed, we will from now on assume that the elastic constants are the same in the two phases.

In the absence of volume forces, the two-dimensional stress tensor can be expressed via an Airy stress function  $\chi$ . Setting

$$\sigma_{xx} = \frac{\partial^2 \chi}{\partial z^2}, \quad \sigma_{xz} = -\frac{\partial^2 \chi}{\partial z \partial x}, \quad \sigma_{zz} = \frac{\partial^2 \chi}{\partial x^2}, \quad (23)$$

we automatically satisfy the condition of mechanical equilibrium  $\sum_j \partial \sigma_{ij} / \partial x_j = 0$ . Hooke's law together with the assumption of isotropic elastic properties then implies that  $\chi$  must obey the biharmonic equation  $\Delta^2 \chi = 0$ . We split the Airy function according to  $\chi(x, z) = \chi^{(0)}(x, z) + \chi^{(1)}(x, z)$ , where

$$\chi^{(0)}(x, z) = -\frac{pl}{2} x^2 + \frac{\sigma_0 - pl}{2} z^2, \quad (24)$$

$$\chi^{(1)}(x, z) = \sum_{n=1}^{\infty} (A_n z + B_n) e^{K_n z} e^{iK_n x} + c.c., \quad (25)$$

$K_n = 2\pi n/\lambda$ , and both terms are solutions to the biharmonic equation separately.

Equation (24) corresponds to a homogeneous stress state and (25) describes the deviation therefrom. Once we have calculated the coefficients  $A_n$ ,  $B_n$  we are able to compute the stress term in (6). Inserting our boundary conditions for the stress field into a representation

of  $\sigma_{nn}$  and  $\sigma_{nt}$  in the  $xz$  coordinate sytem, we arrive at an infinite linear system of equations that in principle could be solved for the coefficients. An analytic result can be obtained, if the equations are expanded in terms of  $\Delta_{\alpha/\beta} = 2h_{\alpha/\beta}/\lambda_{\alpha/\beta}$ , where  $\lambda_\alpha = \eta\lambda$  and  $\lambda_\beta = (1-\eta)\lambda$  are the widths of the lamellas and  $h_\alpha$  ( $h_\beta$ ) is the height of the triangle in the  $\alpha$  ( $\beta$ ) phase (Fig. 5). If the expansion is performed up to linear order, one arrives at

$$A_n = -\sigma_0\lambda e^{-i\pi n\eta} \Delta_{\alpha\beta}^n(\eta), \quad B_n = 0, \quad (26)$$

where

$$\begin{aligned} \Delta_{\alpha\beta}^n(\eta) = & \delta_{n,0} \left( -\Delta_\alpha \frac{\eta}{2} + \frac{1}{4} \Delta_\alpha \eta^2 + \frac{1}{4} \Delta_\beta (1-\eta)^2 \right) \\ & + (1 - \delta_{n,0}) \frac{1}{2\pi^2 n^2} \\ & [\Delta_\alpha + \Delta_\beta (-1)^n - (\Delta_\alpha + \Delta_\beta) \cos(\pi n \eta)]. \end{aligned} \quad (27)$$

Note that in (26) we need this definition only for  $n > 0$ , where it simplifies to the second term. Using these coefficients in  $\chi$  and calculating the average of  $(\sigma_{tt} - \sigma_{nn})^2$ , we obtain

$$\langle (\sigma_{tt} - \sigma_{nn})^2 \rangle_\alpha = \sigma_0^2 \left[ 1 - \frac{1}{\eta} \Omega(\eta) \right], \quad (28)$$

$$\langle (\sigma_{tt} - \sigma_{nn})^2 \rangle_\beta = \sigma_0^2 \left[ 1 + \frac{1}{(1-\eta)} \Omega(\eta) \right], \quad (29)$$

where

$$\Omega(\eta) = 16 \sum_{n=1}^{\infty} \sin(\pi n \eta) \Delta_{\alpha\beta}^n(\eta). \quad (30)$$

To be consistent, we have to compute the average of the diffusion field for the double triangular surface as well. It turns out that the result can be cast into a form that is very similar to the case of a planar interface. All that has to be done is to replace the Jackson-Hunt function  $P(\eta)$  by

$$\begin{aligned} P(\eta, \Delta_\alpha, \Delta_\beta) = & P(\eta) + \frac{2}{\pi^2} \sum_{n=1}^{\infty} \frac{\sin \pi n \eta}{n} \\ & \sum_{m=1}^{\infty} \frac{\sin \pi n \eta m}{m} (\Delta_{\alpha\beta}^{n-m}(\eta) - \Delta_{\alpha\beta}^{n+m}(\eta)), \end{aligned} \quad (31)$$

and here all integer values, including zero, can appear in the superscript of  $\Delta_{\alpha\beta}^{n-m}(\eta)$ . Whereas  $P(\eta)$  is essentially independent of  $\lambda$ , the wavelength dependence of  $\eta$  being weak,  $P(\eta, \Delta_\alpha, \Delta_\beta)$  does depend on the wavelength via the  $\lambda$  dependence of the  $\Delta_{\alpha/\beta}$ . This must be taken into account in the minimization procedure when the minimum undercooling is determined.

Thus replacing  $P(\eta)$  with  $P(\eta, \Delta_\alpha, \Delta_\beta)$  in (8) and (9), we can proceed in a pretty straightforward manner. First we use an assumption analogous to the equal undercooling assumption to eliminate the term  $\frac{1}{k}(c_\infty + \delta + \eta - 1)$

from the formulas. In particular, we assume  $\langle \zeta \rangle_\alpha - \langle \zeta \rangle_\beta = \frac{1}{2}(h_\alpha - h_\beta)$ . Next, we write down the total average undercooling. In minimizing it, we suppose a weak  $\lambda$  dependence of  $\eta$ , which yields  $\partial P(\eta, \Delta_\alpha, \Delta_\beta)/\partial \lambda = -P_1(\eta, \Delta_\alpha, \Delta_\beta)/\lambda$  with  $P_1(\eta, \Delta_\alpha, \Delta_\beta) \equiv P(\eta, \Delta_\alpha, \Delta_\beta) - P(\eta)$ . We then find that, surprisingly, the result for the wavelength does not contain the modified Jackson-Hunt function anymore but just the original one:

$$\begin{aligned} \lambda_{\min}^2 = & \frac{l}{P(\eta)} \{ d_0^\alpha (1-\eta) \sin \vartheta_\alpha + d_0^\beta \eta \sin \vartheta_\beta \\ & + \frac{1}{2} (\eta H^\beta - (1-\eta) H^\alpha) \tilde{\Omega}(\eta) \}, \end{aligned} \quad (32)$$

where

$$\begin{aligned} \tilde{\Omega}(\eta) \equiv \lambda \Omega(\eta) = & 8 \sum_{n=1}^{\infty} \frac{\sin(\pi n \eta)}{\pi^2 n^2} \\ & \left[ \frac{h_\alpha}{\eta} + \frac{h_\beta}{1-\eta} (-1)^n - \left( \frac{h_\alpha}{\eta} + \frac{h_\beta}{1-\eta} \right) \cos(\pi n \eta) \right]. \end{aligned} \quad (33)$$

For comparison with the stress-free case we rewrite this as

$$\lambda_{\min}^2 = \lambda_{\min}^{JH^2}(\eta) \left( 1 + \frac{(\eta H^\beta - (1-\eta) H^\alpha) \tilde{\Omega}(\eta)}{2[d_0^\alpha (1-\eta) \sin \vartheta_\alpha + d_0^\beta \eta \sin \vartheta_\beta]} \right), \quad (34)$$

where we have taken the Jackson-Hunt result for the wavelength at the pertinent value of  $\eta$ . Of course, there is an additional effect (as in Sec. III) due to the change in the volume fraction under external stress. The latter is given by

$$\begin{aligned} \Delta \eta = & \frac{k}{l_T^\alpha + l_T^\beta} \left\{ (l_T^\beta H^\beta - l_T^\alpha H^\alpha) + \frac{1}{2} (h_\beta - h_\alpha) \right. \\ & + \left( \frac{l_T^\beta}{1-\eta} - \frac{l_T^\alpha}{\eta} \right) \frac{2\lambda}{l} P_1(\eta, \Delta_\alpha, \Delta_\beta) \\ & \left. + \Omega(\eta) \left( \frac{l_T^\beta}{1-\eta} H^\beta + \frac{l_T^\alpha}{\eta} H^\alpha \right) \right\}. \end{aligned} \quad (35)$$

In order to get an estimate of the order of magnitude of elastic effects, we note that for  $\sigma_0 \approx 1$  bar and the material parameters considered in section III, we have  $H^{\alpha/\beta} \approx 2 \times 10^{-5}$ .  $\Omega(\eta)$  is on the order of ten, hence  $\tilde{\Omega}(\eta) \approx \lambda$ , if we take the heights  $h^{\alpha/\beta}$  of the lamellas to be of order  $\lambda/10$ . Assuming  $d_0^{\alpha/\beta} \approx 10^{-3}\lambda$ , we find that the second term in (34) is on the order of one percent for  $\sigma_0 = 1$  bar, i.e., an appreciable effect may be expected for pressures or tensions in excess of 10 bar.

With the same assumptions, we note that the change of  $\eta$  induced by elastic effects is on the order of  $10^{-4}$  for  $\sigma_0 = 1$  bar and  $10^{-2}$  for  $\sigma_0 = 10$  bar, hence negligible in most cases in comparison with the direct effect given by

(34). Of course, this also depends on the size of  $d\lambda_{\min}^{JH}/d\eta$ , which we have estimated to be small for  $\eta$  values not too close to 0 or 1, in Sec. III.

We now consider a few special cases that are especially transparent.

If the lamella structure is symmetric under an exchange of the  $\alpha$  and  $\beta$  phases, i.e.,  $\eta = \frac{1}{2}$  and  $h_\alpha = h_\beta$ , then we see immediately from (33) that  $\Omega(\eta) = 0$ . Terms with even  $n$  vanish because of the factor  $\sin(\pi\eta n)$ , terms with odd  $n$  produce a factor of zero inside the brackets. Therefore, application of external stress will not alter the wavelength in this case, except possibly via the change in  $\eta$  induced by (35), which is a much smaller effect. Moreover, if we assume the *thermal* properties of the two phases to be the same, i.e.  $l_T^\alpha = l_T^\beta$ ,  $L_\alpha = L_\beta$ , we have  $H^\alpha = H^\beta$  according to (7) (because we took the *elastic* properties of both phases equal from the outset of this section). Therefore, we have  $\Delta\eta = 0$  in this case. The direct effect on  $\lambda$  as described by (34) is then absent even if  $h_\alpha \neq h_\beta$ , although there will be a small shift in  $\eta$ , if the two phases have different heights.

Another simplification arises, if we choose all the properties of the  $\alpha$  and  $\beta$  phases to be equal and set  $\Delta_\alpha = \Delta_\beta \equiv \Delta$  but allow for  $\eta \neq \frac{1}{2}$ . In particular, this means that we assume the heights of the lamellas to be proportional to their widths. We can then evaluate  $\Omega(\eta)$  analytically,

$$\begin{aligned} \Omega(\eta) &= \frac{8\Delta}{\pi^2} \sum_{n=1}^{\infty} \frac{\sin(\pi n \eta)}{n^2} \left[ 1 + (-1)^n - 2 \cos(\pi n \eta) \right] \\ &= \frac{8\Delta}{\pi} \left( \eta \ln 2 + \int_0^\eta dx \ln |\sin(\pi x)| \right), \end{aligned} \quad (36)$$

and it is easy to show that  $(2\eta - 1)\Omega(\eta) \geq 0$ . Therefore, we have an *increase* of the wavelength in this case.

A discussion of the general case is most easily done by numerical evaluation of (32) for a few characteristic sets of parameter values and graphical representation of the result. This is carried out in Fig. 6. We compare the  $\eta$  dependence of the relative change in wavelength for  $\Delta_\alpha = \Delta_\beta$ ,  $\Delta_\alpha = 2\Delta_\beta$  and  $\Delta_\beta = 2\Delta_\alpha$ .  $\Delta_\alpha$  is set to  $1/10$  and the pressure is 25 bar. The diffusion length is taken to be  $l = 10^2\lambda$  and the capillary length  $d_0 = 10^{-3}\lambda$ . The contact angles have been chosen as  $\vartheta_{\alpha/\beta} = \arctan \Delta_{\alpha/\beta}$  in keeping with the spirit of the triangular approximation. It is seen that when there is an asymmetry between the lamellas, a decrease of the wavelength can occur, but the magnitude of the effect is pretty small if  $\Delta_\alpha \approx \Delta_\beta$ .

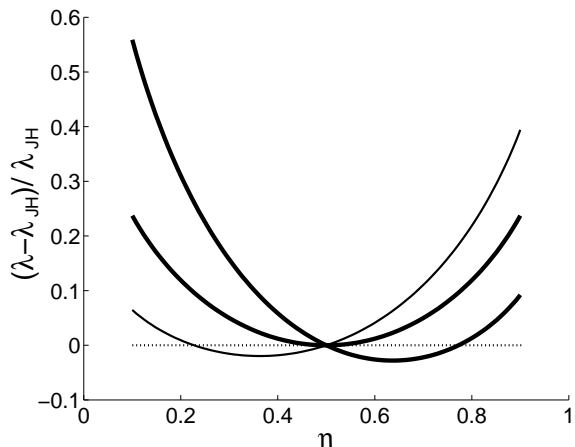


FIG. 6. The change in wavelength  $\lambda$  as a function of the volume fraction  $\eta$  for 25 bar. The thick symmetric curve is for  $\Delta_\alpha = \Delta_\beta = 0.1$ . The thick asymmetric curve is for  $\Delta_\alpha = 0.1$  and  $\Delta_\beta = 0.2$  and the thin curve is for  $\Delta_\alpha = 0.1$  and  $\Delta_\beta = 0.05$ .  $\vartheta_{\alpha/\beta} = \arctan \Delta_{\alpha/\beta}$  is assumed.

## V. SUMMARY

To conclude, motivated by the fact that the interaction between the Grinfeld and Mullins-Sekerka instabilities is strong in directional solidification of dilute alloys [7,8], we were led to investigate the influence of uniaxial stress in directional solidification of lamellar eutectics.

From the outset, two differences could be expected. First, the basic lamellar structure is not determined by the MS instability, so direct visibility of an interaction with the ATG instability was not likely. Second, since the lamellar spacing is typically an order of magnitude smaller than cell spacings in dilute alloys, the influence of the ATG instability which at typical thermal gradients is “resonant” with the MS instability should be expected to be weaker in eutectics.

On the other hand, it is also known that qualitative features that are present in dilute alloys, such as parity breaking or the appearance of asymmetric cells, invariably turn up in eutectics, too, albeit often via a different mechanism, which is a rather fascinating phenomenon by itself. Parity breaking, for example, can be explained by two-mode coupling in cellular growth but requires quite a different analytic approach in the case of eutectics [13]. More basic features, such as the underlying symmetries, are the same in the two cases.

A similar situation arises here: The mechanism, by which stress modifies the properties of the system is entirely different from that of the dilute-alloy case. There it was the coupling to the MS instability, here it is a coupling to *the asymmetry between the two solid phases*. Uniaxial stress has a direct effect on the volume fraction of the phases, which in general results in a (small) influence on the wavelength of the pattern. In addition, it

changes the undercooling of the front in a wavelength-dependent manner, provided there is a (geometric) difference between the  $\alpha$  and  $\beta$  phases. Both effects were calculated to linear order in the deviation  $\Delta$  of the front shape from planarity. The first effect is present even for a planar interface, if the elastic constants of the two solid phases differ, and it has been evaluated for that case as well.

As expected, appreciable wavelength changes require stresses that exceed those necessary in dilute alloys by an order of magnitude. So we do not expect elastic effects to strongly affect directional solidification experiments with eutectics by accident (which might however happen for dilute-alloy experiments). Nevertheless, stresses of 25 bar or so are not too high to be imposed in a controlled experiment which then would allow to test this theory.

Another point worth mentioning is that the wavelength change can be both positive and negative for eutectics (and is positive most of the time) whereas we have only seen a wavelength decrease with dilute alloys so far (at small pulling velocities, the case considered here). This makes the effect somewhat less interesting for material processing purposes but underlines the basic difference in the mechanisms by which stress modifies microstructures in the two cases. Large stresses ( $> 100$  bar), however, might be used to engineer the volume fraction of the phases – if they can be sustained in an appropriate experimental setup.

This work was supported by a 'PROCOPE' grant in the framework of a French-German cooperation.

*els for microstructure and phase transitions*, Lectures at the C.I.M.E. summer school *Calculus of variations and geometric evolution problems*, Cetraro, 1996

- [12] What happens physically, if we try to impose an external stress in the  $x$  direction that is different from the one giving rise to a homogeneous solution, is an altogether different matter. Normally, we then have to deal with the aforementioned free-boundary problem. Physically, it is of course also possible that the coherence of the lamellar interfaces gets lost, i.e., the solid phases may slip on each other, which may strongly modify the local crystal structure.
- [13] A. Valance, C. Misbah, D. Temkin, K. Kassner, *Phys. Rev. E* **48**, 1924 (1993).

- 
- [1] R. J. Asaro and W. A. Tiller, *Metall. Trans.* **3**, 1789 (1972).
- [2] R. H. Torii and S. Balibar, *J. Low Temp. Phys.* **89**, 391 (1992).
- [3] M. A. Grinfeld, *Doklady Akademii Nauk SSSR* **265** 836 (1982); M. A. Grinfeld, *Sov. Phys. Dokl.* **31**, 831 (1986); M. A. Grinfeld, *Europhys. Lett.* **22**, 723 (1993), and references therein.
- [4] P. Nozières, in *Solids Far from Equilibrium*, edited by C. Godrèche (Cambridge University Press, Cambridge, 1992) p. 1.
- [5] P. Nozières, *J. Phys. I, France* **3**, 681 (1993).
- [6] W. W. Mullins and R. F. Sekerka, *J. Appl. Phys.* **35**, 444 (1964).
- [7] I. Durand, K. Kassner, C. Misbah, and H. Müller-Krumbhaar, *Phys. Rev. Lett.*, **76**, 3013 (1996)
- [8] I. Cantat, K. Kassner, C. Misbah, and H. Müller-Krumbhaar, *Phys. Rev. E*, in press.
- [9] K. A. Jackson and J. D. Hunt, *Trans. Metall. Soc. AIME* **236**, 1129 (1966).
- [10] K. Kassner, C. Misbah, *Phys Rev A*, **44**, 6513 (1991).
- [11] S. Müller, private communication and *Variational mod-*